Synthesis and Characterization by ^{19}F and ^{125}Te NMR and Raman Spectroscopy of *cis*-$ReO_2(OTeF_5)_3$ and *cis*-$ReO_2(OTeF_5)_4^-$, and X-ray Crystal Structure of $[N(CH_3)_4^+][$*cis*-$ReO_2(OTeF_5)_4^-]$†

William J. Casteel, Jr., Dianne M. MacLeod, Hélène P. A. Mercier, and Gary J. Schrobilgen*

Department of Chemistry, McMaster University, Hamilton, Ontario L8S 4M1, Canada

Received May 22, 1996⊗

The pentafluorooxotellurate compound $ReO_2(OTeF_5)_3$ has been synthesized from the reaction of ReO_2F_3 with $B(OTeF_5)_3$ and structurally characterized in solution by ^{19}F and ^{125}Te NMR spectroscopy and in the solid state by Raman spectroscopy. The NMR and vibrational spectroscopic findings are consistent with a trigonal bipyramidal arrangement in which the oxygen atoms and an $OTeF_5$ group occupy the equatorial plane. The ^{19}F and ^{125}Te NMR spectra show that the axial and equatorial $OTeF_5$ groups of $ReO_2(OTeF_5)_3$ are fluxional and are consistent with intramolecular exchange by means of a pseudorotation. The Lewis acid behavior of $ReO_2(OTeF_5)_3$ is demonstrated by reaction with $OTeF_5^-$. The resulting *cis*-$ReO_2(OTeF_5)_4^-$ anion was characterized as the tetramethylammonium salt in solution by ^{19}F and ^{125}Te NMR spectroscopy and in the solid state by Raman spectroscopy and X-ray crystallography. The compound crystallizes in the triclinic system, space group $P\bar{1}$, with $a = 13.175(7)$ Å, $b = 13.811(5)$ Å, $c = 15.38(1)$ Å, $\alpha = 72.36(5)^o$, $\beta = 68.17(5)^o$, $\gamma = 84.05(4)^o$, $V = 2476(2)$ Å^3, $D_{calc} = 3.345$ g cm^{-3}, $Z = 4$, $R = 0.0547$. The coordination sphere about Re^{VII} in *cis*-$ReO_2(OTeF_5)_4^-$ is a pseudooctahedron in which the Re−O double bond oxygens are *cis* to one another.

Introduction

The pentafluorooxotellurate ($OTeF_5$) group resembles fluorine in its ability to stabilize the high oxidation states of the elements and is illustrated by the preparation of a considerable number of metal and non-metal $OTeF_5$ derivatives in their highest oxidation states for which the corresponding fluorides are known, e.g., $Xe(OTeF_5)_6$,[1] $Te(OTeF_5)_6$,[2] $U(OTeF_5)_6$,[3] $M(OTeF_5)_6^-$ (M = As, Sb, Bi),[4] $Ti(OTeF_5)_4$,[5] and $Fe(OTeF_5)_3$.[6] The high-valent pentafluorooxotellurate derivatives of the second- and third-row transition metals are limited to $Mo(OTeF_5)_6$,[7] $MoO(OTeF_5)_4$,[7,8] $W(OTeF_5)_6$,[8] $W(OTeF_5)_5$,[7] $WO(OTeF_5)_4$,[7] $OsO(OTeF_5)_4$,[8] $ReO(OTeF_5)_4$,[9] $ReO(OTeF_5)_5$,[9] and $ReO_2(OTeF_5)_3$.[8] Unlike the fluorine-bridged structures of $MoOF_4$,[10] WOF_4,[11] WF_5,[12] $OsOF_4$,[13] and $ReOF_4$,[14] the $OTeF_5$ analogs are not associated by means of bridges involving the $OTeF_5$ ligands.

The highest oxidation state of a metal stabilized by the $OTeF_5$ group is the +7 oxidation state of rhenium. In the present work, we have undertaken to enlarge upon the known $OTeF_5$ derivatives of Re^{VII}. Oxidation of $ReO(OTeF_5)_4$ with $Xe(OTeF_5)_2$ produces $ReO(OTeF_5)_5$ and the crystal structure of $ReO(OTeF_5)_5$, shows octahedral Re coordination with one Re−O double bond[9] and is analogous to the pseudooctahedral structure of $ReOF_5$. The compound $ReO_2(OTeF_5)_3$ was previously reported as the product of the reaction of ReF_7 with $B(OTeF_5)_3$ (eq 1);[8] however, room-temperature Raman and ^{19}F NMR spectra did not provide for a definitive assignment of the structure.

$$ReF_7 + {}^5/_3B(OTeF_5)_3 \rightarrow ReO_2(OTeF_5)_3 + {}^5/_3BF_3 + 2TeF_6 \quad (1)$$

The present work reports the syntheses of $ReO_2(OTeF_5)_3$ from ReO_2F_3 and the *cis*-$ReO_2(OTeF_5)_4^-$ anion as its $N(CH_3)_4^+$ salt, and their structural characterization in solution by ^{19}F and ^{125}Te NMR spectroscopy and in the solid state by Raman spectroscopy. The crystal structure of $[N(CH_3)_4^+][$*cis*-$ReO_2(OTeF_5)_4^-]$ is also reported.

Results and Discussion

Preparation of $ReO_2(OTeF_5)_3$ and $[N(CH_3)_4^+][$*cis*-$ReO_2(OTeF_5)_4^-]$. The compound $ReO_2(OTeF_5)_3$ was previously reported as the product of the reaction of ReF_7 with $B(OTeF_5)_3$,[8] which was a yellow liquid having a melting point of −63.5 °C. The spectroscopy in this work was, however, inconclusive. While the Raman spectrum of $ReO_2(OTeF_5)_3$ was consistent with a nonlinear ReO_2 moiety, the ^{19}F NMR spectrum of the neat liquid showed only a single ("degenerate") AB_4 pattern at room temperature such as would be expected if the oxygen atoms of the ReO_2 moiety were *trans* to each other. Although the $^1J(^{123,125}Te-^{19}F_B)$ coupling was reported, $^1J(^{123,125}Te-^{19}F_A)$ and $^2J(^{19}F_A-^{19}F_B)$ were not reported. The two results appear to be incompatible if the compound possesses either a square pyramidal or a trigonal bipyramidal *cis*-dioxo geometry, since both structural alternatives should show two AB_4 patterns in their ^{19}F NMR spectra having relative intensity ratios of 2:1, and suggest rapid intramolecular exchange of $OTeF_5$ groups on the NMR time scale.

⊗ Abstract published in *Advance ACS Abstracts,* November 15, 1996.

† Dedicated to Professor Karl O. Christe on the occasion of his 60th birthday.

(1) Lentz, D.; Seppelt, K. *Angew. Chem, Int. Ed. Engl.* **1979**, *16*, 729.
(2) Lentz, D.; Pritzkow, H.; Seppelt, K. *Angew. Chem., Int. Ed. Engl.* **1977**, *89*, 741.
(3) Seppelt, K. *Chem. Ber.* **1976**, *109*, 1046.
(4) Mercier, H. P. A.; Sanders, J. C. P.; Schrobilgen, G. J. *J. Am. Chem. Soc.* **1994**, *116*, 2921.
(5) Schröder, K.; Sladky, F. *Chem. Ber.* **1980**, *113*, 1414.
(6) Drews, T.; Seppelt, K. *Z. Anorg. Allg. Chem.* **1991**, *606*, 201.
(7) Turowsky, L.; Seppelt, K. *Z. Anorg. Allg. Chem.* **1990**, *590*, 23.
(8) Huppmann, P.; Labischinski, H.; Lentz, D.; Pritzkow, H.; Seppelt, K. *Z. Anorg. Allg. Chem.* **1982**, *487*, 7.
(9) Turowsky, L.; Seppelt, K. *Z. Anorg. Allg. Chem.* **1990**, *590*, 37.
(10) Edwards, A. J.; Steventon, B. R. *J. Chem. Soc. A* **1968**, 2507.
(11) Edwards, A. J.; Jones, G. R. *J. Chem. Soc. A* **1968**, 2074.
(12) Schroeder, J. *Chem. Ber.* **1970**, *103*, 1536.
(13) Falconer, W. E.; Burbank, R. D.; Jones, G. R.; Sunder, W. A.; Vasile, M. J. *J. Chem. Soc., Chem. Commun.* **1972**, 1080.
(14) Edwards, A. J.; Jones, G. R. *J. Chem. Soc. A* **1968**, 2513.

S0020-1669(96)00597-6 CCC: $12.00

Table 1. ^{19}F and ^{125}Te NMR Data for $ReO_2(OTeF_5)_3$ and *cis*-$ReO_2(OTeF_5)_4^-$

	chemical shifts, ppm[a]			coupling constants, Hz[a]		
	$\delta(^{19}F_A)$	$\delta(^{19}F_B)$	$\delta(^{125}Te^{VI})$	$^2J(^{19}F_A-^{19}F_B)$	$^1J(^{125}Te-^{19}F_A)$	$^1J(^{125}Te-^{19}F_B)$
			$ReO_2(OTeF_5)_3$[b]			
$(OTeF_5)_a$	-45.4	−47.7	566.7	184	3575	3672
$(OTeF_5)_e$	-42.2	−43.5	579.7	185	3480	3598
			$ReO_2(OTeF_5)_4^-$ [c]			
$(OTeF_5)_c$	-41.6	−49.3	564.4	184	3427	3628
$(OTeF_5)_t$	−35.6	−44.5	580.0	184	3224	3549

[a] Spectra were recorded in SO_2ClF at −60 °C. The axial and equatorial environments of the $OTeF_5$ groups are designated by A and B, respectively. [b] The subscripts refer to the axial (a) (*cis* to Re═O bonds) and the equatorial (e) (oxygen bonded to a Te and coplanar with the ReO_2 group) $OTeF_5$ groups in the trigonal bipyramidal $ReO_2(OTeF_5)_3$ molecule. [c] The subscripts denote $OTeF_5$ groups that are *trans* (t) and *cis* (c) to the Re═O bonds.

A new preparation of $ReO_2(OTeF_5)_3$ was carried out by the reaction of ReO_2F_3 with $B(OTeF_5)_3$ in Freon-114 at room temperature according to eq 2. The product was a yellow-green

$$ReO_2F_3 + B(OTeF_5)_3 \xrightarrow{\text{Freon-114}} ReO_2(OTeF_5)_3 + BF_3 \quad (2)$$

liquid with a melting point above 0 °C, which was found to readily supercool to temperatures as low as −78 °C. The $OTeF_5^-$ acceptor abilities of this neutral species were investigated by the interaction of stoichiometric amounts of $[N(CH_3)_4^+][OTeF_5^-]$ and $ReO_2(OTeF_5)_3$ in SO_2ClF, leading to the preparation of $[N(CH_3)_4^+][ReO_2(OTeF_5)_4^-]$ according to eq 3.

$$ReO_2(OTeF_5)_3 + [N(CH_3)_4^+][OTeF_5^-] \xrightarrow{SO_2ClF} [N(CH_3)_4^+][ReO_2(OTeF_5)_4^-] \quad (3)$$

Characterization of $ReO_2(OTeF_5)_3$ and $[N(CH_3)_4^+][$*cis*-$ReO_2(OTeF_5)_4^-]$ by ^{19}F and ^{125}Te NMR Spectroscopy. $ReO_2(OTeF_5)_3$. The ^{19}F NMR data for $ReO_2(OTeF_5)_3$ in SO_2ClF solvent are given in Table 1. The low-temperature (−60 °C) ^{19}F NMR spectrum of $ReO_2(OTeF_5)_3$ (Figure 1a) consists of two second-order AB_4 spin patterns in the ratio of 2:1 [$J_{AB}/\delta\nu_{AB}$ are 0.303 for $(OTeF_5)_e$ and 0.167 for $(OTeF_5)_a$], which are characteristic of $OTeF_5$ groups,[4,15−17] and are assigned to the fluorine ligands of the axial and equatorial $OTeF_5$ ligands, respectively. In contrast, the spectrum at 30 °C (Figure 1b) is broad, consisting of two AB_4 patterns which have begun to coalesce and indicates that $ReO_2(OTeF_5)_3$ undergoes an intramolecular exchange of $OTeF_5$ groups which likely takes place by means of a Berry pseudorotation and is common for trigonal bipyramidal systems.[18] The low-temperature ^{19}F NMR spectrum establishes the *cis* arrangement of the double-bonded oxygen ligands, since the *trans*-dioxo isomer would have only one $OTeF_5$ environment and a single AB_4 pattern in the ^{19}F NMR spectrum. The chemical shifts and $^2J(^{19}F_A-^{19}F_B)$ values for these resonances all fall within the range for other $OTeF_5$ derivatives.[4,15,16,19] The spectrum also displays ^{125}Te and ^{123}Te satellites flanking the main resonances. Unlike ReO_2F_3, which is a fluorine-bridged polymer in the solid state, the geometry deduced for $ReO_2(OTeF_5)_3$ is consistent with a five-coordinate monomeric species. Although the two possible five-coordinate structures, a trigonal bipyramid or a square pyramid, differ little in energy,[20] the trigonal bipyramid is the geometry

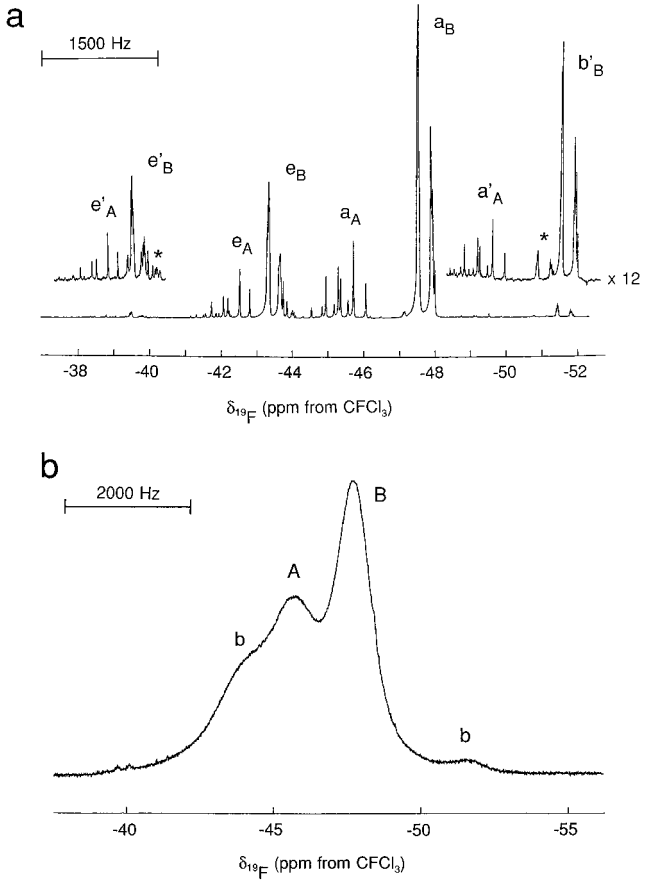

Figure 1. Fluorine-19 NMR spectra (470.599 MHz) of $ReO_2(OTeF_5)_3$ in SO_2ClF: (a) Spectrum recorded at −60 °C showing the fluorine resonances of the axial (a) and equatorial (e) $OTeF_5$ groups, where subscripts A and B denote the axial and equatorial fluorine resonances of the equatorial and axial $OTeF_5$ groups, respectively, primes indicate satellites resulting from the couplings $^1J(^{19}F_A-^{125}Te)$ and $^1J(^{19}F_B-^{125}Te)$, and asterisks denote ^{123}Te satellites where they can be observed; (b) spectrum recorded at 30 °C, where A and B denote the partially exchange-averaged equatorial fluorines of the axial and equatorial $OTeF_5$ groups, respectively, and peaks denoted by b are ^{125}Te satellites arising from coupling to the equatorial fluorines of the equatorial $OTeF_5$ groups, $^1J(^{125}Te-^{19}F_B)$. The weaker and broadened axial fluorine resonances of the $OTeF_5$ groups are obscured by the broad equatorial fluorine resonances of the axial and equatorial $OTeF_5$ groups.

which is most commonly observed for main-group and d^0 five-coordinate systems.[21] The structure of monomeric ReO_2F_3 has been studied by matrix-isolation infrared and Raman spectroscopy and shown to have a trigonal bipyramidal geometry.[22] More recently, local density and nonlocal density functional

(15) Collins, M. J.; Schrobilgen, G. J. *Inorg. Chem.* **1985**, *24*, 2608.
(16) Birchall, T.; Myers, R. D.; DeWaard, H.; Schrobilgen, G. J. *Inorg. Chem.* **1982**, *21*, 1068.
(17) Emsley, J. W.; Feeney, J.; Sutcliffe, L. H. *High Resolution Nuclear Magnetic Resonance Spectroscopy*; Pergamon Press: New York, 1965; Vol. 1, Chapter 8, pp 337−340 and Appendix F.
(18) Berry, R. S. J. *Chem. Phys.* **1960**, *32*, 933.
(19) Mercier, H. P. A.; Sanders, J. C. P.; Schrobilgen, G. J. *Inorg. Chem.* **1995**, *34*, 5261.
(20) Gillespie, R. J.; Hargittai, I. *The VSEPR Model of Molecular Geometry*; Allyn and Bacon: Boston, MA, 1991; pp 58−60.
(21) Cotton, F. A.; Wilkinson, G. *Advanced Inorganic Chemistry*, 5th ed.; J. Wiley & Sons: New York, 1988; Chapter 19.

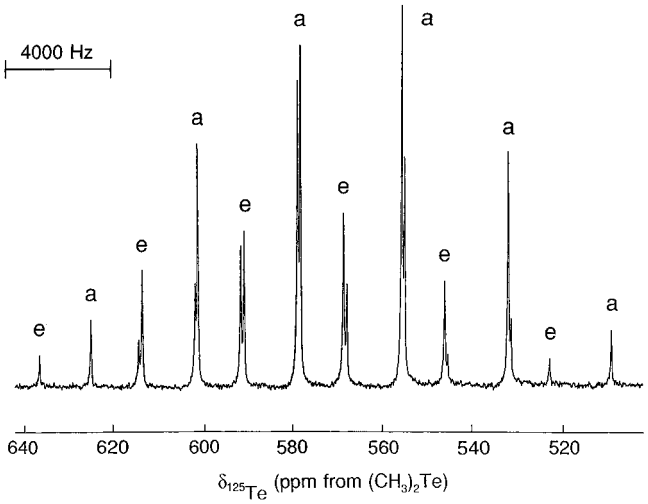

Figure 2. Tellurium-125 NMR spectrum (157.791 MHz) of $ReO_2(OTeF_5)_3$ in SO_2ClF at −60 °C consisting of two overlapping doublets of quintets arising from the equatorial (e) $OTeF_5$ group and the axial (a) $OTeF_5$ groups.

theory calculations have confirmed trigonal bipyramidal C_{2v} geometries for ReO_2F_3 and the isoelectronic $OsO_2F_3^+$ cation.[23] The structure of $ReO_2(OTeF_5)_3$ is therefore expected to be closely related to the structures of these species and is likewise assigned a trigonal bipyramidal geometry in which the double bond oxygen atoms occupy the equatorial plane (structure **I**).

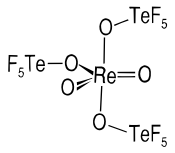

I

The ^{125}Te chemical shifts for $ReO_2(OTeF_5)_3$ in SO_2ClF at −60 °C are given in Table 1 and occur in the region typically observed for Te^{VI} and other $OTeF_5$ derivatives.[4,15,16,19] The ^{125}Te NMR spectrum of $ReO_2(OTeF_5)_3$ in SO_2ClF (Figure 2) appears as two sets of overlapping doublets of quintets having a relative intensity ratio of 2:1 which is consistent with a trigonal bipyramidal geometry. The spin coupling patterns arise from $^1J(^{125}Te-^{19}F_A)$ and $^1J(^{125}Te-^{19}F_B)$ of the two axial $OTeF_5$ groups and the one equatorial $OTeF_5$ group. Slight multiplet asymmetries arise from higher order effects of the AB_4 portions of the $^{125}TeAB_4$ spin systems.[15,16]

In both the ^{19}F and ^{125}Te NMR spectra of $ReO_2(OTeF_5)_3$, the chemical shift(s) of the equatorial $OTeF_5$ group occur to higher frequency when compared to those of the axial $OTeF_5$ groups. The deshielding of the fluorine ligands and tellurium of the equatorial $OTeF_5$ group relative to those of the axial $OTeF_5$ group implies that the axial Re−O bonds of the oxo bridges are more ionic than the equatorial Re−O bonds and is in accord with other trigonal bipyramidal species where the more ionic (electronegative) ligand occupies the axial position(s) of a trigonal bipyramid.[20] The ordering of chemical shifts is presumably reinforced by pπ-dπ bonding because the p-orbitals of the oxygen of the equatorial $OTeF_5$ group compete for the same d-orbitals as the double bond oxygens.

$[N(CH_3)_4^+][cis\text{-}ReO_2(OTeF_5)_4^-]$. The ^{19}F NMR data for $[N(CH_3)_4^+][cis\text{-}ReO_2(OTeF_5)_4^-]$ in SO_2ClF solvent are given in Table 1, and the spectrum of the $cis\text{-}ReO_2(OTeF_5)_4^-$ anion is shown in Figure 3 and consists of two sets of essentially first order doublets and quintets and establishes the *cis* geometry of the pseudooctahedral anion in solution. The spectrum exhibits some asymmetry in the multiplets, as well as some splitting of the quintets which arise from second-order effects so that the spectrum is best described as two AB_4 spin systems which are near first order [$J_{AB}/\delta\nu_{AB}$ are 0.0439 for $(OTeF_5)_t$ and 0.0512 for $(OTeF_5)_c$]. In addition, the AB_4 patterns in the ^{19}F spectrum are flanked by ^{125}Te and ^{123}Te satellites. The ^{125}Te chemical shifts for $cis\text{-}ReO_2(OTeF_5)_4^-$ in SO_2ClF at −60 °C are given in Table 1. The ^{125}Te NMR spectrum of $cis\text{-}ReO_2(OTeF_5)_4^-$ in SO_2ClF (Figure 4) appears as two overlapping doublets of quintets in the fluorine-on-tellurium region arising from coupling of ^{125}Te to the ^{19}F ligands of the two $OTeF_5$ groups that are *cis* to each other but *trans* to the oxygen double bonds and of the two $OTeF_5$ groups that are *trans* to each other.

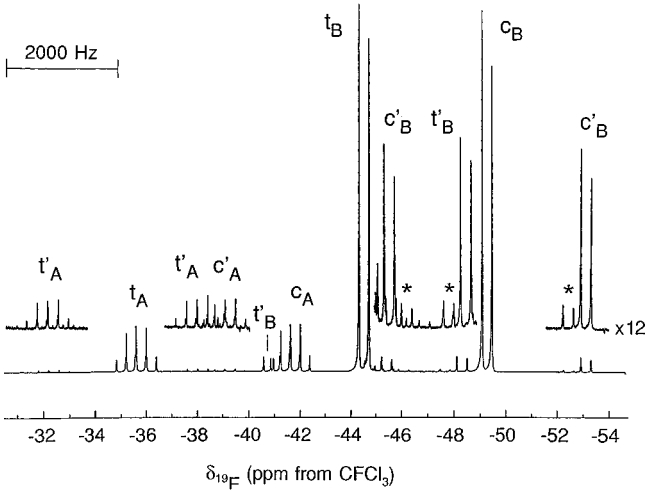

Figure 3. Fluorine-19 NMR spectrum (470.599 MHz) of $[N(CH_3)_4^+]$-$[cis\text{-}ReO_2(OTeF_5)_4^-]$ in SO_2ClF at −60 °C. The $OTeF_5$ groups which are *trans* to Re═O but *cis* to each other are denoted by t, and those which are *cis* to Re═O and *trans* to each other are denoted by c. The subscripts denote the axial (A) and equatorial (B) fluorine environments of the $OTeF_5$ groups, primes denote ^{125}Te satellites arising from the couplings $^1J(^{125}Te-^{19}F_A)$ and $^1J(^{125}Te-^{19}F_B)$, and asterisks denote ^{123}Te satellites where they can be observed.

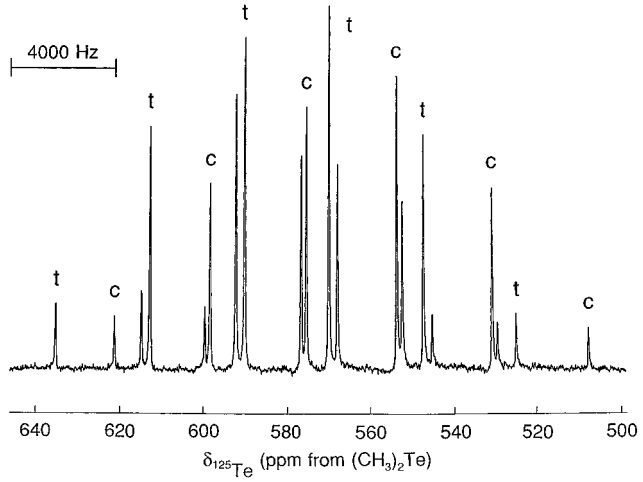

Figure 4. Tellurium-125 NMR spectrum (157.791 MHz) of $[N(CH_3)_4^+]$-$[cis\text{-}ReO_2(OTeF_5)_4^-]$ in SO_2ClF at −60 °C showing two overlapping doublets of quintets arising from the ^{125}Te atoms on the $OTeF_5$ groups which are (t) *trans* to Re═O and *cis* to each other and (c) *cis* to Re═O and *trans* to each other.

Unlike those for $ReO_2(OTeF_5)_3$, the absolute assignments of the ^{19}F and ^{125}Te chemical shifts to $OTeF_5$ groups that are *cis*

(22) Beattie, I. R.; Crocombe, R. A.; Ogden, J. S. *J. Chem. Soc., Dalton Trans.* **1977**, 1481.
(23) Casteel, W. J., Jr.; Mercier, H. P. A.; Dixon, D. A.; Schrobilgen, G. J. *Inorg. Chem.* **1996**, *35*, 4310.

Table 2. Summary of Crystal Data and Refinement Results for $[N(CH_3)_4^+][cis\text{-}ReO_2(OTeF_5)_4^-]$

empirical formula	$C_4H_{12}F_{20}NO_6ReTe_4$
space group	$P\bar{1}$
unit cell dimensions	$a = 13.175(7)$ Å, $b = 13.811(5)$ Å, $c = 15.380(10)$ Å, $\alpha = 72.36(5)°$, $\beta = 68.17(5)°$, $\gamma = 84.05(4)°$
V	2476(2) Å^3
molecules/unit cell	4
mol wt	1246.75
calcd density	3.345 g cm^{-3}
T	−48 °C
μ	5.176 mm^{-1}
wavelength	0.560 86 Å
final agreement factors[a]	$R_1 = 0.0547$, w$R_2 = 0.1419$

[a] R_1 is defined as $\sum||F_o| - |F_c||/\sum|F_o|$. w$R_2 = (\sum w(F_o^2 - F_c^2)^2/\sum w|F_o|^2)^{1/2}$.

or *trans* to the Re═O bonds in the *cis*-$ReO_2(OTeF_5)_4^-$ anion are ambiguous. A rationale based on the relative Te−O σ-bond characters of the *cis*- and *trans*-$OTeF_5$ groups provides an ordering of the ^{19}F and ^{125}Te chemical shifts. The $OTeF_5$ groups that are *trans* to one another and *cis* to Re═O bonds are assigned to low frequency of $OTeF_5$ groups that are *trans* to Re═O bonds. The π-character of the Re−O bond of the Te−O−Re oxo-bridge is diminished by the *trans* influence of the Re═O bond and results in enhancement of the Re−O σ-bond characters by inductively withdrawing electron density from the TeF_5 group. The resulting enhanced inductive effect of the oxygen serves to deshield the ^{19}F and ^{125}Te environments of the *trans*-$OTeF_5$ groups relative to those of the *cis*-$OTeF_5$ groups. The axial $^{125}Te-^{19}F$ couplings are significantly smaller than their equatorial counterparts and parallel the relative Te−F bond lengths (see **X-ray Crystal Structure of $[N(CH_3)_4^+][cis\text{-}ReO_2(OTeF_5)_4^-]$**). However, the $^{125}Te-^{19}F$ couplings of the *trans*-$OTeF_5$ groups are significantly smaller and are consistent with inductive withdrawal of s-electron density from the *trans*-TeF_5 groups. The chemical shift and $^{125}Te-^{19}F$ coupling constant trends for the *cis*-$ReO_2(OTeF_5)_4^-$ anion are also consistent with the observations that the ^{19}F and ^{125}Te chemical shifts of the equatorial $OTeF_5$ group of $ReO_2(OTeF_5)_3$ are deshielded relative to those of the axial $OTeF_5$ groups, and the $^{125}Te-^{19}F$ coupling of the equatorial $OTeF_5$ group is significanlty less than that of the axial $OTeF_5$ groups (*vide supra*).

X-ray Crystal Structure of $[N(CH_3)_4^+][cis\text{-}ReO_2(OTeF_5)_4^-]$. Details of the data collection parameters and other crystallographic information are given in Table 2. The final atomic coordinates and the equivalent isotropic thermal parameters are summarized in Table 3. Important bond lengths and bond angles for the *cis*-$ReO_2(OTeF_5)_4^-$ anion are listed in Table 4.

The structure of $[N(CH_3)_4^+][cis\text{-}ReO_2(OTeF_5)_4^-]$ consists of well-separated anions and cations. The tetramethylammonium cations are tetrahedral about nitrogen with the expected bond lengths and bond angles. Besides $ReO(OTeF_5)_5$, the *cis*-$ReO_2(OTeF_5)_4^-$ anion is only the second example of an $OTeF_5$ derivative of Re^{VII} that has been characterized by X-ray crystallography. Of the two crystallographically independent *cis*-$ReO_2(OTeF_5)_4^-$ anions, the Re(1) anion is better defined than the Re(2) anion, which displays larger thermal parameters. However, the bond lengths and angles in both anions are equal within experimental error after correction for libration (in the text, the values related to the Re(2) anion appear in square brackets). The geometry of the anion is pseudooctahedral around the rhenium atom and is in accord with the *cis* geometry deduced from the solution ^{19}F and ^{125}Te NMR studies (see **Characterization by ^{19}F and ^{125}Te NMR Spectroscopy**). The two axial positions are occupied by two $OTeF_5$ groups, while the equatorial positions are occupied by two $OTeF_5$ groups and two oxygen atoms that are *cis* to one another (Figure 5).

The $O_{eq}-Re-O_{eq}$ and $O_{ax}-Re-O_{ax}$ single-bond angles of *cis*-$ReO_2(OTeF_5)_4^-$ are significantly smaller than 90 and 180°, respectively, and can be rationalized in terms of double-bond domain−single bond domain repulsions predicted by the VSEPR rules.[20] The axial $O_{ax}-Re-O_{ax}$ angle is bent toward the two oxygens of the equatorial $OTeF_5$ groups, and away from the Re═O bonds in the same equatorial plane (O(1)−Re(1)−O(2), 163.0(4)° [O(6)−Re(2)−O(7), 163.2(8)°]), and even more severe compressions are observed for the $O_{eq}-Re-O_{eq}$ angles (O(3)−Re(1)−O(4), 77.1(3)° [O(5)−Re(2)−O(8), 74.8(5)°]).

With the exception of those of the ReO_6^{5-} anion (Li^+ salt),[24] which is expected to have a high degree of charge localization on the oxygen atoms (1.886(3) Å), the Re═O bond lengths of *cis*-$ReO_2(OTeF_5)_4^-$ (1.664(9) [1.654(11)] Å) are comparable to those in other pseudooctahedral Re^{VII} species reported in the literature: *cis*-$ReO_2F_4^-$ (1.678(9) Å),[25] $ReO(OTeF_5)_5$ (1.68(1) Å),[9] $ReOF_5$ (1.642(40) Å),[26] Re_2O_7 (1.65(3)−1.73(3) Å)[27] and to those of the pentagonal bipyramidal $ReOF_6^-$ anion (1.629(14)−1.671(7) Å)[28] and is longer than the Re^{VI}═O bond in $ReO(OTeF_5)_4\cdot F_2Te(OTeF_5)_2$ (1.63(7) Å).[9] As expected, the $Re-O_t$ bonds (2.053(8) [2.027(10)] Å) *trans* to the Re═O bonds in the *cis*-$ReO_2(OTeF_5)_4^-$ anion are longer than the $Re-O_c$ bonds (1.940(8) [1.907(13)] Å) *cis* to the Re═O bonds. The $Re-O_t$ bond is comparable to the $Re-O_t$ bond *trans* to the Re═O bond in $ReO(OTeF_5)_5$ (1.96(1) Å), which is also longer than the $Re-O_c$ bonds (1.88(1) Å). This trend is also observed for *cis*-$ReO_2F_4^-$, where the $Re-F_t$ bond (2.002(7) Å) is longer than the $Re-F_c$ bond (1.867(8) Å), and for the pseudooctahedral ReO_6 moiety of Re_2O_7, where the oxo-bridged $Re-O_t$ bonds are 2.09(3)−2.16(3) Å (average 2.13(3) Å) and the oxo-bridged $Re-O_c$ bonds are 1.73(2)−1.75(2) and 2.05(2)−2.08(2) Å (average 1.90(2) Å).

Transition elements in the second and third rows of the periodic table prefer octahedral coordination of ligands, and it has been found that octahedral dioxo compounds of transition metals in the d^0 state prefer a *cis* arrangement of the oxygen ligands.[29] The exclusive preference for the *cis* arrangement is also seen for TcO_2F_3,[30] $TcO_2F_4^-$,[31] $ReO_2F_4^-$,[25] $Re_3O_6F_{10}^-$,[25] OsO_2F_4,[32] and $Os_2O_4F_7^+$,[23] which exist as the *cis*-dioxo isomers, and is explained by the strong oxygen to metal $p\pi \rightarrow d\pi$ bonding. In *cis*-$ReO_2(OTeF_5)_4^-$ and related d^0 *cis*-MO_2F_4 species, each oxygen atom of the *cis*-ReO_2 moiety possesses two filled p-orbitals available for π-bonding with the empty set of metal $d_{t_{2g}}$ orbitals. In the *trans* isomer the two donating p-orbitals on both oxygen atoms must compete for the same two $d_{t_{2g}}$ orbitals having the correct symmetry for overlap. In the *cis* isomer, all three $d_{t_{2g}}$ orbitals are available for overlap. The result is that the bonding molecular orbitals in the *cis* isomer have lower energies than the bonding molecular orbitals in the *trans* isomer resulting in a *cis* isomer that is more stable.

(24) Betz, T.; Hoppe, R. *Z. Anorg. Allg. Chem.* **1984**, *512*, 19.
(25) Casteel, W. J., Jr.; Dixon, D. A.; LeBlond, N.; Lock, P. E.; Mercier, H. P. A.; Schrobilgen, G. J. *Inorg. Chem.* 1996 submitted.
(26) Alekseichuk, I. S.; Ugarov, V. V.; Sokolov, V. B.; Rambidi, N. G. *Zh. Strukt. Khim.* **1981**, *22*, 182.
(27) Krebs, B.; Müller, A.; Beyer, H. H. *Inorg. Chem.* **1969**, *8*, 436.
(28) Giese, S.; Seppelt, K. *Angew. Chem., Int. Ed. Engl.* **1994**, *33*, 461.
(29) (a) Cotton, F. A.; Morehouse, S. M.; Wood, J. S. *Inorg. Chem.* **1964**, *3*, 1603. (b) Blake, A. B.; Cotton, F. A.; Wood, J. S. *J. Am. Chem. Soc.* **1964**, *86*, 3024.
(30) Mercier, H. P.; Schrobilgen, G. J. *Inorg. Chem.* **1993**, *32*, 145.
(31) Dixon, D. A.; LeBlond, N.; Mercier, H. P. A.; Schrobilgen, G. J. *Inorg. Chem.* **1996** submitted.
(32) Christe, K. O.; Dixon, D. A.; Mack, H. G.; Oberhammer, H; Pagelot, A.; Sanders, J. C. P.; Schrobilgen, G. J. *J. Am. Chem. Soc.* **1993**, *115*, 11279.

Table 3. Atomic Coordinates ($\times 10^4$) and Equivalent Isotropic Displacement Parameters ($A^2 \times 10^3$) for $[N(CH_3)_4^+][cis\text{-}ReO_2(OTeF_5)_4^-]$

	x	y	z	U(eq)[a]
Re(1)	2745(1)	7049(1)	6995(1)	38(1)
O(10)	1609(8)	6360(8)	7616(7)	62(2)
O(11)	2551(8)	7927(7)	7588(7)	58(2)
O(1)	3620(7)	6163(6)	7685(6)	48(2)
Te(1)	3638(1)	4856(1)	8412(1)	37(1)
F(10)	2518(8)	5046(6)	9454(6)	74(3)
F(11)	3658(7)	3559(6)	9165(7)	71(2)
F(12)	4572(8)	5204(6)	8881(8)	81(3)
F(13)	2706(8)	4382(7)	8009(7)	81(3)
F(14)	4778(8)	4531(8)	7450(9)	102(4)
O(2)	2249(8)	7896(6)	5977(7)	52(2)
Te(2)	1727(1)	9170(1)	5627(1)	41(1)
F(20)	2677(7)	9372(7)	4390(6)	70(2)
F(21)	2661(8)	9759(6)	5930(7)	70(2)
F(22)	739(8)	8670(8)	5319(8)	88(3)
F(23)	743(7)	9035(7)	6850(7)	82(3)
F(24)	1194(9)	10424(7)	5227(7)	83(3)
O(3)	4270(6)	7680(6)	6078(5)	41(2)
Te(3)	5505(1)	7974(1)	6186(1)	38(1)
F(30)	6795(7)	8280(7)	6240(6)	70(2)
F(31)	5924(8)	6662(7)	6491(9)	90(3)
F(32)	4920(8)	7900(10)	7472(6)	95(4)
F(33)	6278(7)	8109(8)	4899(6)	75(3)
F(34)	5260(8)	9337(7)	5872(9)	89(3)
O(4)	3291(6)	6192(6)	6047(6)	41(2)
Te(4)	2865(1)	5714(1)	5259(1)	42(1)
F(40)	2869(13)	4428(7)	5972(9)	115(5)
F(41)	1423(7)	5864(9)	5879(8)	91(3)
F(42)	2891(12)	6954(8)	4387(8)	105(4)
F(43)	4279(9)	5611(13)	4485(9)	125(5)
F(44)	2431(9)	5207(8)	4481(8)	88(3)
Re(2)	−1109(1)	11105(1)	9119(1)	39(1)
O(20)	133(8)	10573(9)	8942(9)	72(3)
O(21)	−1806(10)	10470(17)	10235(11)	181(11)
O(5)	−2450(7)	11985(8)	9048(7)	58(2)
Te(5)	−3669(1)	12469(1)	9774(1)	40(1)
F(50)	−4452(10)	12171(14)	9158(13)	165(8)
F(51)	−4946(7)	12968(7)	10481(7)	70(2)
F(52)	−4096(11)	11268(8)	10700(10)	133(6)
F(53)	−3100(8)	12790(11)	10565(9)	107(4)
F(54)	−3430(13)	13758(8)	9001(9)	135(6)
O(6)	−804(10)	12195(13)	9497(14)	131(7)
Te(6)	142(1)	12682(1)	9876(1)	41(1)
F(60)	1017(9)	13202(7)	10293(9)	88(3)
F(61)	1301(8)	11990(11)	9312(10)	117(5)
F(62)	−994(8)	13404(9)	10463(10)	105(4)
F(63)	−129(10)	11664(9)	10966(9)	113(4)
F(64)	499(11)	13764(13)	8822(9)	146(6)
O(7)	−1512(15)	10324(11)	8455(19)	170(10)
Te(7)	−2528(1)	9780(1)	8240(1)	49(1)
F(70)	−2874(8)	11010(7)	7607(7)	74(2)
F(71)	−3473(9)	9216(9)	7924(8)	93(3)
F(72)	−3608(11)	9850(10)	9338(8)	123(5)
F(73)	−1544(10)	9653(10)	7081(11)	124(5)
F(74)	−2271(13)	8510(8)	8876(12)	134(6)
O(8)	−611(11)	12093(13)	7784(8)	118(6)
Te(8)	163(1)	12598(1)	6612(1)	88(1)
F(80)	−584(16)	12160(19)	6093(13)	215(10)
F(81)	−60(14)	13841(10)	6435(21)	252(14)
F(82)	1194(25)	12956(21)	5374(12)	287(15)
F(83)	915(19)	11289(13)	6688(14)	201(10)
F(84)	1298(17)	12838(20)	6940(19)	235(11)
N(1)	4010(7)	11422(7)	7419(7)	37(2)
C(1)	4024(12)	11282(12)	8417(9)	58(3)
C(2)	3208(11)	10731(12)	7474(10)	61(4)
C(3)	3707(16)	12482(10)	7023(12)	73(5)
C(4)	5090(11)	11199(13)	6753(12)	67(4)
N(2)	−1634(8)	16117(8)	7551(7)	42(2)
C(5)	−1845(13)	15660(11)	6874(10)	60(4)
C(6)	−2709(10)	16341(10)	8283(9)	48(3)
C(7)	−1005(13)	17076(12)	6987(13)	74(4)
C(8)	−1004(11)	15379(11)	8104(10)	58(3)

[a] U(eq) is defined as one-third of the trace of the orthogonalized $\mathbf{U}_{ij}$ tensor.

Table 4. Bond lengths (Å) and Angles (deg) for $cis\text{-}ReO_2(OTeF_5)_4^-$

Bond Lengths[a]			
Re(1)−O(10)	1.655(9) [1.660]	Re(1)−O(11)	1.673(9) [1.679]
Re(1)−O(1)	1.944(8) [1.948]	Re(1)−O(2)	1.935(8) [1.939]
Re(1)−O(3)	2.072(8) [2.079]	Re(1)−O(4)	2.034(8) [2.041]
mean Te−O	1.814(8) [1.816]	mean Te−F	1.811(8) [1.816]
Re(2)−O(21)	1.624(12) [1.634]	Re(2)−O(20)	1.684(10) [1.692]
Re(2)−O(5)	2.056(8) [2.066]	Re(2)−O(6)	1.896(12) [1.901]
Re(2)−O(7)	1.918(13) [1.923]	Re(2)−O(8)	1.998(12) [2.011]
mean Te−O	1.76(1) [1.77]	mean Te−F	1.80(1) [1.81]

Bond Angles			
O(10)−Re(1)−O(11)	101.9(5)	O(10)−Re(1)−O(2)	95.7(5)
O(11)−Re(1)−O(2)	95.0(4)	O(10)−Re(1)−O(1)	95.6(4)
O(11)−Re(1)−O(1)	95.2(4)	O(2)−Re(1)−O(1)	163.0(4)
O(10)−Re(1)−O(4)	91.4(4)	O(11)−Re(1)−O(4)	166.5(4)
O(2)−Re(1)−O(4)	81.6(3)	O(1)−Re(1)−O(4)	85.4(3)
O(10)−Re(1)−O(3)	168.3(4)	O(11)−Re(1)−O(3)	89.6(3)
O(2)−Re(1)−O(3)	84.8(4)	O(1)−Re(1)−O(3)	81.6(3)
O(4)−Re(1)−O(3)	77.1(3)	Te(1)-O(1)-Re(1)	139.8(4)
Te(2)−O(2)−Re(1)	139.0(5)	Te(3)−O(3)−Re(1)	137.9(4)
Te(4)−O(4)−Re(1)	141.2(4)	O(21)−Re(2)−O(20)	102.2(7)
O(21)−Re(2)−O(6)	93.4(11)	O(20)−Re(2)−O(6)	95.8(5)
O(21)−Re(2)−O(7)	98.3(12)	O(20)−Re(2)−O(7)	93.4(6)
O(6)−Re(2)−O(7)	163.2(8)	O(21)−Re(2)−O(8)	165.1(7)
O(20)−Re(2)−O(8)	92.7(6)	O(6)−Re(2)−O(8)	83.6(8)
O(7)−Re(2)−O(8)	82.0(9)	O(21)−Re(2)−O(5)	90.3(6)
O(20)−Re(2)−O(5)	167.4(5)	O(6)−Re(2)−O(5)	81.2(5)
O(7)−Re(2)−O(5)	86.8(5)	O(8)−Re(2)−O(5)	74.8(5)
Te(5)−O(5)−Re(2)	143.0(5)	Te(6)−O(6)−Re(2)	144.8(7)
Te(7)−O(7)−Re(2)	150.5(13)	Te(8)−O(8)−Re(2)	158.9(9)

[a] Distances after corrections for thermal motion by the riding model are given in square brackets.

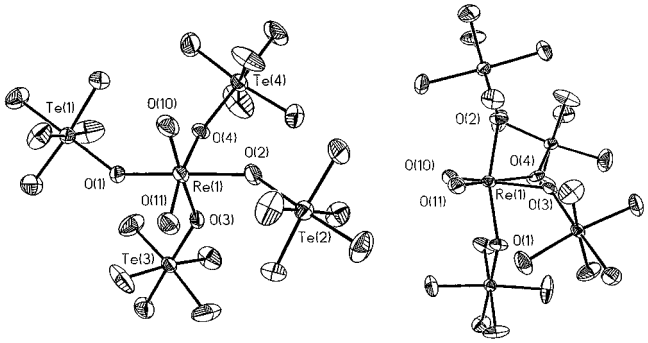

Figure 5. ORTEP views of the $cis\text{-}ReO_2(OTeF_5)_4^-$ anion in $[N(CH_3)_4^+][cis\text{-}ReO_2(OTeF_5)_4^-]$ (thermal ellipsoids shown at the 50% probability level).

Another result of the strong oxygen−metal $p\pi \rightarrow d\pi$ bonding is that the M−O(F) bonds which are *trans* to the M═O bonds are longer and weaker than the M−O(F) bonds *cis* to M═O bonds. The *cis*-dioxo preference is not seen with the main-group elements. The VSEPR rules would predict a *trans* arrangement of the doubly bonded oxygen domains to be more stable if d orbital participation were not involved.[20] This contrasts with the geometry of the $IO_2F_4^-$ anion,[33] which exists as a mixture of *cis* and *trans* isomers having a *cis*/*trans* ratio largely determined by kinetic factors.

The environment around each Te^{VI} atom is octahedral, with the Te^{VI}−O (1.814(8) [1.76(1)] Å) and Te^{VI}−F (1.811(8) [1.80(1)] Å) bond lengths in agreement with values reported for other $OTeF_5$ compounds.[1−9,19]

The anions and cations are packed along the *b* axis so that two stacks of Re(1) and Re(2) anions form a channel with the cations surrounding this channel (Figure 6). The relative

(33) Christe, K. O.; Wilson, R. D.; Schack, C. J. *Inorg. Chem.* **1981**, *20*, 2104.

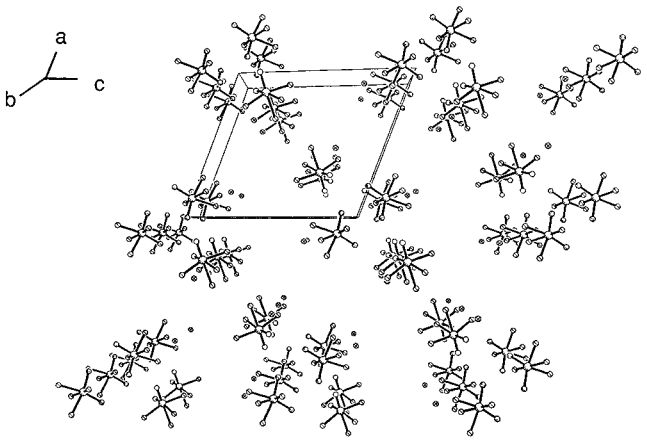

Figure 6. View of the $[N(CH_3)_4^+][cis\text{-}ReO_2(OTeF_5)_4^-]$ unit cell showing the packing along the *b* axis. For clarity, the F, C and H atoms have been omitted.

orientations of the Re(1) and Re(2) anions are such that all the Re═O bonds point toward the interior of the channel. The $Re(1)O_2$ and $Re(2)O_2$ planes form a dihedral angle of ~90°. Each Re(1) anion has six anion−cation contacts (range 2.980−3.294 Å) which are significantly smaller than the sum of the $CH_3\cdots F$ van der Waals radii (3.35[34] −3.40[35] Å), whereas each Re(2) anion has five longer anion−cation contacts (range 3.189−3.305 Å). The longer $CH_3\cdots F$ contacts may account for the larger anisotropy observed in the Re(2) anions, whereas the Re(1) anions are much more constrained due to shorter $CH_3\cdots F$ contacts.

Characterization of $ReO_2(OTeF_5)_3$ and $[N(CH_3)_4^+][cis\text{-}ReO_2(OTeF_5)_4^-]$ by Raman Spectroscopy. The solid state Raman spectra of the title compounds are shown in Figure 7, and the frequencies and their assignments are given in Tables 5 and 6. The Raman frequencies of liquid $ReO_2(OTeF_5)_3$ were previously reported,[8] but no assignments were given. Spectral assignments are tentative owing to uncertainties regarding the degree of vibrational coupling among the $OTeF_5$ modes of the ligands, the degree of site symmetry lowering, as well as vibrational coupling within the unit cells (factor-group splitting). A factor-group analysis correlating the C_1 point symmetry of the free $cis\text{-}ReO_2(OTeF_5)_4^-$ anion to the crystallographic site symmetry (C_i) and to the symmetry of the unit cell (C_i) reveals that each vibrational mode should appear as two Raman-active A_g and two infrared-active A_u components under the crystal symmetry. In the majority of cases, modes which are formally singly degenerate under their local assigned symmetries do not exhibit factor-group splittings, and it may be concluded that the anions are weakly coupled.

The stretching vibrations of the Re═O bonds give two strong and characteristic bands in the Raman spectra of the title compounds, consistent with the *cis*-dioxo geometries of these two compounds. For a bent O═Re═O moiety, two Raman-active Re═O stretching modes are expected, whereas *trans*-dioxo arrangements would be expected to give only one Raman active Re═O stretching mode. The symmetric Re═O stretches are at higher frequency than the asymmetric stretches, and in the case of $ReO_2(OTeF_5)_3$, these assignments are confirmed by polarization measurements on the liquid compound (Figure 7b). This differs from what is seen in main-group systems such as $cis\text{-}IO_2F_4^-$,[33] but it is seen with other d^0 transition metal derivatives containing *cis*-dioxo arrangements such as TcO_2F_3,[30] ReO_2F_3,[22,23] $OsO_2F_3^+$,[23] $cis\text{-}ReO_2F_4^-$,[25,36] $cis\text{-}OsO_2F_4$,[32] and $cis\text{-}TcO_2F_4^-$.[31] The symmetric and factor-group-split asymmetric ReO_2 stretches of $cis\text{-}ReO_2(OTeF_5)_3$ are observed at 1028 and 974 and 970 cm^{-1}, respectively, and have been assigned by comparison with those of matrix-isolated ReO_2F_3 at 1026 and 990 cm^{-1}.[22] The symmetric and asymmetric ReO_2 stretches of $cis\text{-}ReO_2(OTeF_5)_4^-$ are observed at 992 and 952 cm^{-1}, respectively, and have been assigned by comparison with those of Li^+ (1011, 973 cm^{-1}),[25] Na^+ (1011, 973 cm^{-1}),[25] K^+ (987, 951 cm^{-1}),[36] and Cs^+ (973, 940 cm^{-1})[25] salts of the $cis\text{-}ReO_2F_4^-$ anion. The remaining modes associated with the $O_2ReO_{2t}O_c$ moiety of $ReO_2(OTeF_5)_3$ and the $O_2ReO_{2t}O_{2a}$ moiety of the $ReO_2(OTeF_5)_4^-$ anion have been tentatively assigned under C_{2v} point symmetry by analogy with the assignments for matrix-isolated ReO_2F_3,[22,23] the $cis\text{-}ReO_2F_4^-$ anion,[25,36] and $cis\text{-}OsO_2F_4$.[32] Their respective vibrational representations are $5A_1 + A_2 + 3B_1 + 3B_2$ and $6A_1 + 2A_2 + 3B_1 + 4B_2$, and all are Raman and infrared active. The assignments of these modes are not discussed further, but the frequency assignments of the model compounds have been previously confirmed by *ab initio* calculations.

The remaining frequency assignments of the frequencies of the $OTeF_5$ group have been aided by comparison with the assignments for $[N(CH_3)_4^+][TeOF_5^-]$,[37] which have been confirmed by *ab initio* calculations and a normal-coordinate analysis, and with the assignments for F_5TeOF,[38] and F_5TeOCl.[38] Assignments for the $OTeF_5$ groups were made under local point symmetry C_{4v}, which results in 15 vibrations, $4A_1 + 2B_1 + B_2 + 4E$, all of which are Raman active (A_1 and E are infrared active) and require no further discussion. The Re−O stretches of the Re−O−Te bridges are tentatively assigned to bands in the 890−920 cm^{-1} region and are to high frequency of the Te−O stretches. Tentative assignments for the Re−O−Re bridge in Re_2O_7 have been reported to occur at 800 and 830 cm^{-1} although several bands are also reported in the 857−1006 cm^{-1} region.[39] Bands attributable to Te−O stretching modes have been observed for $M(OTeF_5)_6^-$ (M = Nb,[40] Ta,[40] As,[4] Sb,[4] Bi[4]) anions at 800−900 cm^{-1}.

The assignments for the $N(CH_3)_4^+$ cation of $[N(CH_3)_4^+][cis\text{-}ReO_2(OTeF_5)_4^-]$ are based on those for the free $N(CH_3)_4^+$ cation,[4,19,41,42] which belongs to the point group T_d and has 19 fundamental vibrational bands, $3A_1 + A_2 + 4E + 4T_1 + 7T_2$, of which the A_1, E, and T_2 modes are Raman active and the T_2 modes are infrared active. The assignments for the cation generally follow those previously given for other $N(CH_3)_4^+$ salts and require no further commnent.

CONCLUSIONS

The synthesis of $ReO_2(OTeF_5)_3$ from pure ReO_2F_3 and $B(OTeF_5)_3$ was carried out, and the product was characterized by ^{19}F and ^{125}Te NMR spectroscopy as well as by Raman spectroscopy. The $ReO_2(OTeF_5)_3$ molecule was shown to be fluxional on the NMR time scale, which is consistent with a trigonal bipyramid in which the oxygen atoms occupy the equatorial plane. At room temperature, the $OTeF_5$ groups undergo slow intramolecular exchange by means of a pseu-

(34) Pauling, L. *The Nature of the Chemical Bond*, 3rd ed.; Cornell University Press: Ithaca, NY, 1960; p 260.
(35) Bondi, A. *J. Phys. Chem.* **1964**, *68*, 441.
(36) Kuhlmann, W.; Sawodny, W. *J. Fluorine Chem.* **1977**, *9*, 341.
(37) Christe, K. O.; Dixon, D. A.; Sanders, J. C. P.; Schrobilgen, G. J.; Wilson, W. W. *Inorg. Chem.* **1993**, *32*, 4089.
(38) Christe, K. O.; Schack, C. J.; Wilson, W. W. *Inorg. Chem.* **1983**, *22*, 18.
(39) Krebs, B.; Müller, A. *Z. Naturforsch.* **1968**, *23B*, 415.
(40) Moock, K.; Seppelt, K. *Z. Anorg. Allg. Chem.* **1988**, *561*, 132.
(41) (a) Kabisch, G.; Klose, M. *J. Raman Spectrosc.* **1978**, *7*, 311. (b) Kabisch, G. *J. Raman Spectrosc.* **1980**, *9*, 279.
(42) Wilson, W. W.; Christe, K. O.; Feng, J.; Bau, R. *Can. J. Chem.* **1989**, *67*, 1898.

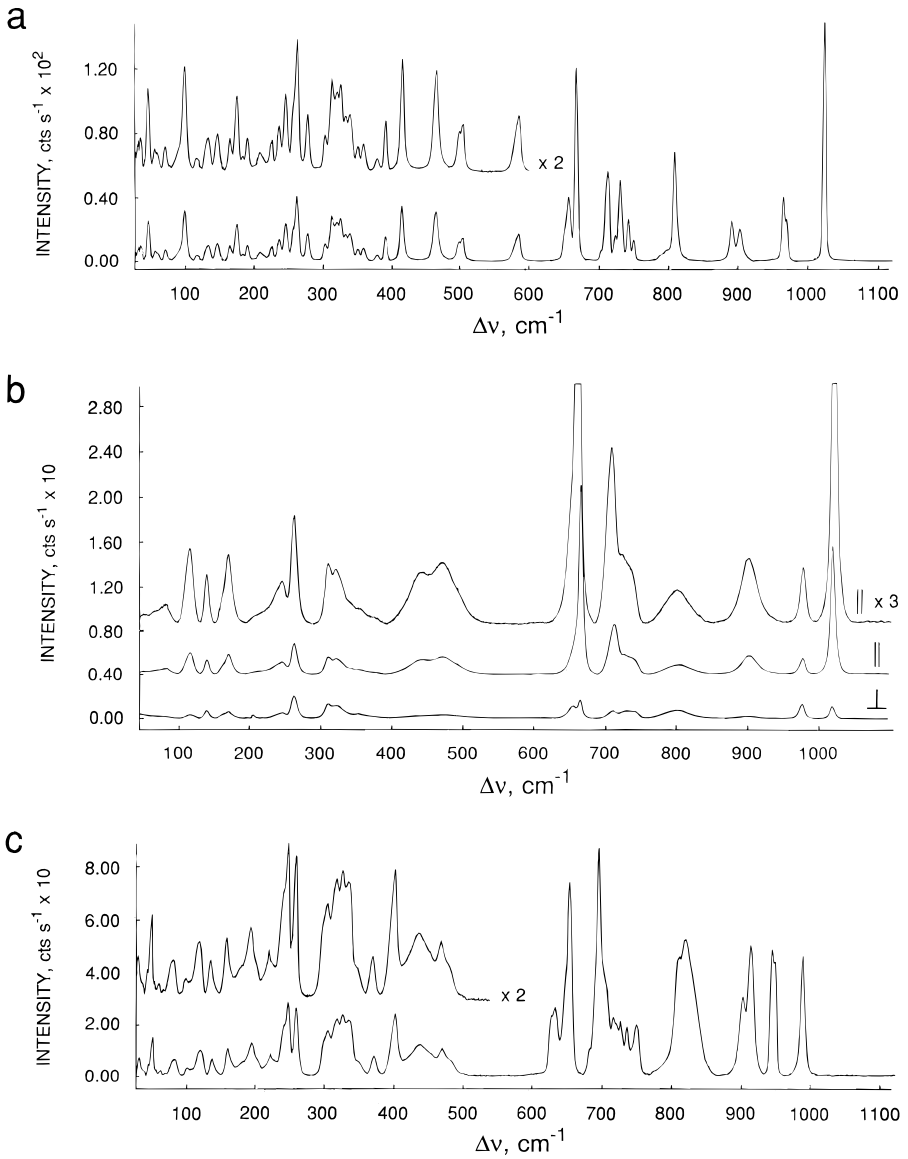

Figure 7. Raman spectra of (a) microcrystalline (−100 °C) and (b) liquid (22 °C) $ReO_2(OTeF_5)_3$ where ∥ and ⊥ are the parallel and perpendicular components, respectively, of the Stokes lines and (c) microcrystalline $[N(CH_3)_4^+][cis\text{-}ReO_2(OTeF_5)_4^-]$ (−130 °C) recorded in Pyrex glass tubes using 514.5-nm excitation.

dorotation mechanism. The acceptor properties of the neutral compound with respect to the $OTeF_5^-$ anion were explored, leading to the synthesis of the *cis*-$ReO_2(OTeF_5)_4^-$ anion as the tetramethylammonium salt. The anion was characterized by X-ray crystallography, ^{19}F and ^{125}Te NMR spectroscopy, and Raman spectroscopy and shown to have approximately octahedral coordination around rhenium and to exclusively exist as the *cis*-dioxo isomer in solution and in the solid state.

Experimental Section

Materials and Apparatus. All manipulations of air-sensitive compounds were carried out under anhydrous conditions in a two-station nitrogen atmosphere drybox (Vacuum Atmospheres Model DLX). In the case of volatile fluorides, manipulations were carried out on a vacuum line constructed of 316 stainless steel, nickel, Teflon, and FEP. Pressures were measured with the use of an MKS Model PDR-5B power supply and digital readout in conjunction with MKS pressure transducers (0−1000 Torr) which had inert, wetted Inconel surfaces. A Pyrex vacuum line was used for vacuum-drying FEP reactors and for transferring Freon-114 and SO_2ClF.

All preparative work was carried out in lengths of $^3/_8$ in. o.d. FEP tubing fused to lengths of $^1/_4$ in. FEP tubing. One end of the $^3/_8$ in. o.d. FEP tube was heat sealed, and the other end was connected through a 45° SAE flare to a Kel-F valve. All reactors previously dried on a Pyrex vacuum line, were transferred to a metal vacuum line, where they were passivated with F_2 at 1 atm for several hours, evacuated, and back-filled with N_2 before being transferred to the drybox for use.

Materials which were purified or prepared by standard literature methods were ReO_2F_3,[25] SO_2ClF (Columbia Organic Chemical Co.),[43] Freon-114 (Aldrich), $B(OTeF_5)_3$,[4] and $[N(CH_3)_4^+][OTeF_5^-]$.[4]

Preparation of $ReO_2(OTeF_5)_3$. In the drybox, 1.14 905 g (4.1753 mmol) of ReO_2F_3 was weighed into a $^3/_8$ in. o.d FEP reactor. Freon-114 (ca. 5 mL) was condensed onto ReO_2F_3 at approximately −196 °C on a Pyrex vacuum line. In a cold well cooled to −196 °C and located in the floor of the drybox, the Freon-114 solution was frozen, and 3.0554 g (4.205 mmol) of $B(OTeF_5)_3$ was then added onto the mixture. The reaction vessel was closed with a Kel-F valve, removed from the drybox, attached to the Pyrex vacuum line while still cold, and evacuated at −196 °C. Upon warming to −78 °C and then gradually to 0 °C, BF_3 evolution commenced and the soluton changed from colorless to light yellow. The reaction mixture was warmed to room temperature, and BF_3 was periodically pumped off after cooling the reaction mixture to −78 °C. During reaction, several heads of volatile material from the reaction were condensed into a 40 mL

(43) Schrobilgen, G. J.; Holloway, J. H.; Granger, P.; Brevard, C. *Inorg. Chem.* **1978**, *17*, 980.

Table 5. Raman Frequencies and Assignments for $ReO_2(OTeF_5)_3$[a]

frequency, cm^{-1}		assignments[b]	frequency, cm^{-1}		assignments[b]
$ReO_2(OTeF_5)_3$ solid (−100 °C)	$ReO_2(OTeF_5)_3$ liquid (22 °C)	$OTeF_5$ (C_{4v}); O_2ReO_3 (C_{2v})	$ReO_2(OTeF_5)_3$ solid (−100 °C)	$ReO_2(OTeF_5)_3$ liquid (22 °C)	$OTeF_5$ (C_{4v}); O_2ReO_3 (C_{2v})
1028 (100)	1022 (68), p	$\nu_1(A_1)$, ν_s(O═Re═O)	358 (6) 350 (5)	 351, sh, dp	$\nu_{11}(B_2)$, δ_{as}(O═ReO_e + ReO_{2a}) scissor
974 (18), sh 970 (28)	978 (9), dp	$\nu_{10}(B_2)$, ν_{as}(O═Re═O)	339 (12) 332 (11)	338, sh, dp	$\nu_9(E)$, $\delta(FTeF_4)$
916 (3), sh		$\nu_2(A_1)$, $\nu_s(ReO_{2a} + ReO_e)$	325 (18) 320 (17)	319 (8), dp	$\nu_{10}(E)$, $\delta(OTeF_4)$
906 (14)	902 (10), br, p	$\nu_7(B_1)$, $\nu_{as}(ReO_{2a})$	313 (19) 303 (8)	308 (9), dp	$\nu_4(A_1)$, $\delta_s(FTeF_4)$; $\nu_7(B_2)$, $\delta(TeF_4)$ scissor
895 (18)		$\nu_3(A_1)$, $\nu_s(ReO_{2a} - ReO_e)$			
811 (46) 800 (5), sh 791 (4), sh	802 (5), br, dp[c]	$\nu_1(A_1)$, ν(TeO)	277 (12) 262 (27) 256 (14), sh	 260 (16)	$\nu_{11}(E)$, $\delta_{as}(TeF_4)$; $\nu_{11}(B_2)$, δ_{as}(O═ReO_e +ReO_{2a})
751 (9) 743 (18)		$\nu_8(E)$, $\nu_{as}(TeF_4)$	246 (16) 236 (9) 225 (6)	243 (7), p 236, sh	$\nu_5(A_1)$, δ_s(O═Re═O in plane −O_eReO_a)
732 (34) 725 (11)	737 (8), sh, p 727 (10), sh, p	$\nu_2(A_1)$, ν(TeF)	208 (4)	205 (2), p	δ(Re−O−Te)
714 (38) 704 (5), sh	712 (27), p		190 (7) 183 (3) 174 (16) 163 (6)	 166(11), p	
669 (80)	665 (100), p	$\nu_3(A_1)$, $\nu_s(TeF_4)$			
657 (27) 651 (14), sh	655 (15), sh, dp	$\nu_5(B_1)$, $\nu_{as}(TeF_4)$	145 (8)	158, sh, p	
585 (12)[d] 577 (6), sh		ν(Re---F)	132 (7)	137 (8), dp	$\nu_{12}(B_2)$, δ_{as}(O═ReO_e−ReO_{2a})
			116 (2) 98 (21)	112 (12), p	τ(Re−O−Te)
504 (10) 499 (9)	*e*	$\nu_8(B_1)$, δ_{as}(O_eReO_a in plane)			
			87 (5), sh		lattice mode
465 (21)	469 (9), br, p	$\nu_4(A_1)$, δ(O═Re═O + O_eReO_a) scissor	69 (5)	77 (3), p	τ(Re−O−Te)
415 (23)	440 (8), br, p	$\nu_6(A_2)$, τ(O═Re═O + ReO_{2a})	55 (4) 44 (17) 33 (6)		lattice modes
391 (11) 378 (3)		$\nu_9(B_1)$, δ_{as}(O═Re═O out of plane) 371, sh			

[a] The spectra were recorded on a sample sealed inside a 4-mm Pyrex glass tube using 514.5-nm excitation. Values in parentheses denote relative intensities; sh denotes a shoulder, br a broad band, p a polarized band, and dp a depolarized band. [b] The oxygens of the oxo bridges are denoted by subscripts for those occupying the equatorial plane (e) and axial positions (a) of a trigonal bipyramid. [c] The depolarization of this band is possibly attributed to weak asymmetrical coupling of the axial and equatorial Te−O stretching modes. [d] These bands are not observed in the liquid; see Results and Discussion. [e] Bands may overlap with the broad band at 469 cm^{-1}.

stainless steel Hoke cylinder which was cooled to −78 °C while the FEP reactor was held at 0 °C and shown by gas phase infrared spectroscopy to consist of BF_3 with no detectable amount of TeF_6. After ReO_2F_3 had dissolved and gas evolution had ceased, the solution was yellow to yellow-green and was allowed to stand at room temperature with intermittent agitation for approximately $^1/_2$ hr. The solvent was removed under dynamic vacuum at 0 °C until constant weight was achieved. The final mass of the product was 3.900 g (4.1756 mmol, 100% yield). The product was a pale yellow powder at −78 °C and a yellow to yellow-green liquid at room temperature having a melting point above 0 °C. The liquid was found to supercool readily, preventing the accurate determination of the melting point. The product was stored at −78 °C until used.

Preparation of $[N(CH_3)_4^+][cis\text{-}ReO_2(OTeF_5)_4^-]$. In the drybox, 2.2070 g (2.363 mmol) of $ReO_2(OTeF_5)_3$ was pipetted into a preweighed $^3/_8$ in. o.d. FEP reaction tube. On the Pyrex vacuum line, SO_2ClF (ca. 4 mL) was distilled onto $ReO_2(OTeF_5)_3$ at −196 °C. Using the cold well in the drybox, 0.7315 g (2.339 mmol) of $[N(CH_3)_4^+][OTeF_5^-]$ was added to the frozen solution of $ReO_2(OTeF_5)_3$ in SO_2ClF at approximately −196 °C. Upon warming, all of the $[N(CH_3)_4^+][OTeF_5^-]$ immediately dissolved to give an intense yellow-green solution. The solvent was pumped off at −78 °C, leaving a light yellow solid, and pumping was continued at room temperature for several hours. The solid was recovered in the drybox (2.9238 g, 2.345 mmol; 99.2% yield).

Nuclear Magnetic Resonance Spectroscopy. Nuclear magnetic resonance samples were prepared in either 4 mm o.d. (for ^{19}F) or 9 mm o.d. (for ^{125}Te) FEP tubes for NMR work that had been previously dried under vacuum and passivated for several hours with 1 atm of F_2. Solutes were loaded into the tubes in the dry box, and SO_2ClF solvent was condensed solvent onto the solutes at −196 °C. The sample tubes were heat-sealed under dynamic vacuum, and the sample tubes were stored at −196 °C until their NMR spectra could be obtained. The FEP sample tubes were inserted into 5- or 10-mm precision glass NMR tubes (Wilmad) to record the NMR spectra.

All spectra were recorded unlocked (field drift <0.1 Hz h^{-1}) on a Bruker AM-500 spectrometer equipped with an 11.744-T cryomagnet and an Aspect 3000 computer. Fluorine-19 spectra were acquired with a 5-mm combination $^1H/^{19}F$ probe operating at 470.599 MHz. Free induction decays for ^{19}F were accumulated in 32K memories. A spectral width setting of 20 or 100 kHz was employed, yielding data point resolutions of 1.2 and 6.0 Hz/data point and acquisition times of 0.82 and 0.16 s, respectively. No relaxation delays were applied. Typically, 750−4000 transients were accumulated. The pulse width corresponding to a bulk magnetization tip angle, θ, of approximately 90° was equal to 1 μs. No line-broadening parameters were used in the exponential multiplication of the free induction decays prior to Fourier transformation.

The ^{125}Te spectra were obtained using a 10-mm broad-band probe (tunable over the range 23−202 MHz) which was tuned to 157.794 MHz to observe ^{125}Te. Free induction decays were accumulated in 16 K memories with spectral width settings of 30 or 50 kHz corresponding to acquisition times of 0.28 and 0.16 s and data point resolutions of 3.6 and 6.1 Hz/data point, respectively. No relaxation delays were applied. Typically, 10 000−30 000 transients were accumulated for the ^{125}Te spectra. The pulse width corresponding to a bulk magnetization tip angle, θ, of approximately 90° was 18 μs. Line-broadening parameters used in the exponential multiplication of the free induction decays were 3−7 Hz.

Table 6. Raman Frequencies and Assignments for $[N(CH_3)_4^+][cis\text{-}ReO_2(OTeF_5)_4^-]$[a]

frequency, cm^{-1}	assignments: cation (T_d)	assignments: anion $OTeF_5$ (C_{4v}); O_2ReO_4 (C_{2v})
3061 (13), sh	$\nu_5(E)$, $\nu_{as}(CH_3)$	
3048 (24)	$\nu_{13}(T_2)$, $\nu_{as}(CH_3)$	
2992 (60)	$\nu_1(A_1)$, $\nu_s(CH_3)$	
2982 (9), sh		
2964 (13)	$\nu_{14}(T_2)$, $\nu_{as}(CH_3)$	
2903 (4)		
2874 (3)	$2\nu_6(E)$, $2\nu_2(A_1)$	
2903 (4)		
2874 (3)	$\nu_6(E) + \nu_{16}(T_2)$	
2825 (9)	$2\nu_{16}(T_2)$	
2821 (8), sh		
1487 (1)	$\nu_6(E)$, $\delta_{as}(CH_3)$	
1453 (75)	$\nu_2(A_1)$, $\delta_s(CH_3)$	
1420 (4)	$\nu_{16}(T_2)$, $\delta_{as}(CH_3)$	
1290 (3)	$\nu_{17}(T_2)$, $\delta_{rock}(CH_3)$	
1169 (6)	$\nu_7(E)$, $\delta_{rock}(CH_3)$	
992 (53)		$\nu_1(A_1)$, $\nu_s(O{=}Re{=}O)$
952 (51)[b]		$\nu_{12}(B_2)$, $\nu_{as}(O{=}Re{=}O)$
947 (56)[b]	$\nu_{18}(T_2)$, $\nu_{as}(C_4N)$	
916 (57)		$\nu_9(B_1)$, $\nu_{as}(ReO_{2a})$
904 (36)		$\nu_2(A_1)$, $\nu_s(ReO_{2a} + ReO_{2e})$
821 (60)		$\nu_1(A_1)$, $\nu(Te{-}O)$
812 (53)		
751 (24)		$\nu_8(E)$, $\nu_{as}(TeF_4)$
737 (22)		
727 (25)		$\nu_2(A_1)$, $\nu(TeF)$
722 (24), sh		
716 (27)		
704 (45), sh		
696 (100)		$\nu_{13}(B_2)$, $\nu_{as}(ReO_{2e})$
683 (13), sh		
654 (85)		$\nu_3(A_1)$, $\nu_s(TeF_4)$
646 (40), sh		$\nu_5(B_1)$, $\nu_{as}(TeF_4)$
633 (31)		$\nu_3(A_1)$, $\nu_s(ReO_{2a} - ReO_{2e})$
628 (28), sh		
482 (8), sh		$\nu_4(A_1)$, $\delta(O{=}Re{=}O)$ scissor
468 (13)	$\nu_{19}(T_2)$, $\delta(C_4N)$	
436 (15), br		$\nu_5(A_1)$, $\delta_s(ReO_{2a} + ReO_{2e})$ scissor
402 (28)		$\nu_{14}(B_2)$, $\delta_{as}(O{=}ReO_e + ReO_{2a})$ scissor
371 (10)	$\nu_8(E)$, $\delta(C_4N)$	
350 (7), sh		$\nu_7(A_2)$, $\tau(O{=}Re{=}O)$
335 (26)		$\nu_9(E)$, $\delta(FTeF_4)$
326 (28)		$\nu_{10}(E)$, $\delta(OTeF_4)$
317 (26)		$\nu_6(A_1)$, $\delta_s(ReO_{2a} - ReO_{2e})$ scissor
304 (21)		$\nu_4(A_1)$, $\delta_s(FTeF_4)$;
297 (17), sh		$\nu_7(B_2)$, $\delta(TeF_4)$ scissor
258 (31)		$\nu_{10}(B_1)$, $\delta_{as}(ReO_{2e})$ rock
246 (33)		
240 (24), sh		
220 (7)		
203 (7), sh		$\delta(Re{-}O{-}Te)$
193 (16)		
179 (7)		
158 (13)		$\nu_{15}(B_2)$, $\delta_{as}(O{=}ReO_e - ReO_{2a})$ scissor
135 (8)		$\nu_8(A_2)$, $\tau(ReO_{2e})$
117 (12)		$\tau(Re{-}O{-}Te)$
98 (4)		lattice modes
79 (8)		
58 (3)		
47 (17)		
27 (9)		

[a] Spectrum of a microcrystalline solid in a Pyrex glass tube at −130 °C was recorded using 514.5-nm excitation. Values in parentheses denote relative intensities; sh denotes a shoulder and br a broad band. [b] These bands are nearly coincident and their assignments may be interchanged.

The ^{19}F and ^{125}Te NMR spectra were referenced to external samples of neat $CFCl_3$ and $Te(CH_3)_2$, respectively, at 30 °C. The chemical shift convention used is that a positive (negative) sign indicates a chemical shift to high (low) frequency of the reference compound.

Structure Determination of $[N(CH_3)_4^+][cis\text{-}ReO_2(OTeF_5)_4^-]$. Crystal Growing. Single crystals of $[N(CH_3)_4^+][cis\text{-}ReO_2(OTeF_5)_4^-]$ were grown in a previously vacuum-dried glass vessel equipped with a glass/Teflon valve and a side tube, by warming a saturated SO_2ClF solution of the salt under a partial presence (1 atm) of dry N_2 in the glass vessel. Upon dissolution of the compound at ca. 45−50 °C, the vessel was immersed in a 2-L vessel of water at 50 °C, covered with Styrofoam and allowed to cool over a two day period to room temperature. Clusters of parallelepiped-shaped crystals formed and were isolated by decanting the mother liquor into the side tube of the vessel and slowly removing SO_2ClF under vacuum at 0 °C. The glass vessel was cut open in the drybox, and several crystal fragments were cleaved from the dried clusters and mounted under a microscope in the drybox in dry glass Lindemann capillaries. The crystal used in this study was a parallelepiped with dimensions 0.5 × 0.4 × 0.4 mm.

Collection and Reduction of X-ray Data. The crystal of $[N(CH_3)_4^+][cis\text{-}ReO_2(OTeF_5)_4^-]$ was centered on a Siemens/Syntex $P2_1$ diffractometer using silver radiation monochromatized with a graphite crystal ($\lambda = 0.560\ 86$ Å). Accurate cell dimensions were determined at −48 °C from a least-squares refinement of the setting angles (χ, ϕ, and 2θ) obtained from 26 accurately centered reflections (with $12.47° \le 2\theta \le 27.32°$) chosen from a variety of points in reciprocal space. Integrated diffraction intensities were collected using a $\theta-2\theta$ scan technique with scan rates varying from 3 to 14.65°/min (in 2θ) and a scan range of ±0.45° so that the weaker reflections were examined most slowly to minimize counting errors. The data were collected with $-16 \le h \le 18$, $-20 \le k \le 18$, and $-19 \le l \le 21$ and with $3 \le 2\theta \le 50°$. During data collection, the intensities of three standard reflections were monitored every 97 reflections to check for crystal stability and alignment. Over the course of data collection, no decay was observed. A total of 14 305 reflections were collected. A total of 13 221 unique reflections remained after averaging of equivalent reflections of which 8939 satisfied the condition $I \ge 2\sigma(I)$ and were used for structure solution. Corrections were made for Lorentz and polarization effects, while an empirical absorption correction was applied to the data using the ψ-scan method ($\Delta\phi = 10°$) ($\mu\bar{R} = 1.1137$).

Crystal Data. $C_4H_{12}F_{20}NO_6ReTe_4$ ($f_w = 1246.75$) crystallizes in the triclinic space group, $P\bar{1}$, with $a = 13.175(7)$ Å, $b = 13.811(5)$ Å, $c = 15.380(10)$ Å, $\alpha = 72.36(5)°$, $\beta = 68.17(5)°$, $\gamma = 84.05(4)°$, $V = 2476(2)$ Å^3, and $D_{calc} = 3.345$ g cm^{-3} for $Z = 4$. Ag Kα radiation ($\lambda = 0.560\ 86$ Å, μ(Ag Kα) = 5.176 mm^{-1}) was used.

Solution and Refinement of the Structures. The XPREP program[44] confirmed the original cell and that the lattice was triclinic. The structure was shown to be centrosymmetric by an examination of the *E* statistics (calculated, 0.940, theoretical, 0.968), and consequently the structure was solved in the space group $P\bar{1}$.

The solution was obtained by direct methods, which located the positions of two rhenium and eight tellurium atoms. The full-matrix

least-squares refinement of all these atom positions and isotropic thermal parameters gave a conventional agreement index R_1 ($=\sum||F_o| - |F_c||/\sum|F_o|$) of 0.1919. Successive difference Fourier syntheses revealed the remaining fluorine, oxygen, carbon, and nitrogen atoms, confirming the presence of the *cis*-$ReO_2(OTeF_5)_4^-$ anion and $N(CH_3)_4^+$ cation. Refinement of positional and isotropic temperature parameters for all atoms (d(C−H) = 0.96 Å, U(H) fixed to 0.08) converged at 0.1310. The final refinement was obtained by refining all the atoms of the anion anisotropically, by introducing a weight factor [$w = 1/\sigma^2(F_o^2) + (0.0768P^2) + 9.8022P$] and gave rise to a residual, R_1, of 0.0547 (wR_2 = 0.1419). In the final difference Fourier map, the maximum and minimum electron densities were +6.463 and −7.562 e Å^{-3}.

All calculations were performed on a Silicon Graphics, Inc., Model 4600PC workstation using the SHELXTL PLUS[44] determination package for structure solution, refinement and molecular graphics.

Raman Spectroscopy. Raman spectra were recorded on a Jobin-Yvon Mole S-3000 triple-spectrograph system equipped with 0.32-m prefilter, adjustable 25-mm entrance slit, and a 1.00-m monochromator. The instrument settings for the *cis*-$ReO_2(OTeF_5)_4^-$ anion, when they differ from those of $ReO_2(OTeF_5)_3$, are given in square brackets. Holographic gratings were used for the prefilter (600 grooves mm^{-1}, blazed at 500 nm) and monochromator (1800 grooves mm^{-1}, blazed at 550 nm) stages. The 514.5-nm line of a Spectra Physics Model 2016 Ar^+ ion laser was used for excitation of the samples. Spectra were recorded at −100 °C [−130 °C] on microcrystalline samples and at 22 °C for liquid $ReO_2(OTeF_5)_3$ vacuum-sealed in dry 4 mm o.d. Pyrex glass tubes using the macrochamber of the instrument. Low temperatures were achieved by flowing dry N_2 gas, chilled by passing through a 50-L tank of liquid nitrogen, along the outside of the sample tube, which was mounted vertically in an open-ended unsilvered glass Dewar jacket, and checked by placing a copper−constantan thermocouple wire (error ±0.8 °C) in the sample region. A Spectraview-2D CCD detector equipped with a 25-mm chip (1152 × 298 pixels) was used for signal averaging. The Raman spectrometer was frequency calibrated using the 1018.3 or 730.4 cm^{-1} line of neat indene. The laser power was adjusted to 100−200 mW at the sample, with slit settings corresponding to a resolution of 1 cm^{-1}). A total of 15 reads having 60 s integration times were summed for the Raman spectra of $ReO_2(OTeF_5)_3$ [$ReO_2(OTeF_5)_4^-$]. Depolarization ratios were measured at 90° to the incident plane polarized radiation, and the radiation was scrambled by means of a quartz plate placed immediately after the polarization analyzer.

Acknowledgment. We thank the donors of the Petroleum Research Fund, administered by the American Chemical Society, for support of this work under ACS-PRF Grant No. 26192-AC3. We also thank the National Science Foundation for the award of a NATO Postdoctoral Fellowship to W.J.C.

Supporting Information Available: A structure determination summary (Table 7), anisotropic thermal parameters (Table 8), remaining bond lengths and bond angles (Table 9), and atomic coordinates for the hydrogen atoms (Table 10) of [$N(CH_3)_4^+$][*cis*-$ReO_2(OTeF_5)_4^-$] (7 pages). Ordering information is given on any current masthead page.

IC960597C

(44) Sheldrick, G. M. *SHELXTL PLUS*, Release 4.21/V; Siemens Analytical X-ray Instruments Inc.: Madison, Wisconsin, 1990.